Modified r-Method for the Finite Element Adaptive Analysis of Plane Elastic Problems

Hyung-Seok Oh* and Jang-Keun Lim**

(Received August 25, 1995)

The nodal relocation method (r-method) is used to uniformly distribute element discretization errors over an analytic model and improve the solution quality. When this r-method is performed with Zienkiewicz-Zhu's error estimator, its converged solution can not be easily obtained without many iterative calculations. Further, this method also may deteriorate solution quality because of serious element distortion. This paper suggests a new error estimator which can evaluate the size and the distortion error of an isoparametric element separately and proposes a modified r-method based on this error estimator. Various numerical experiments show that the proposed error estimator properly evaluates the element discretization errors and the modified r-method can be easily applied to the practical analysis owing to the comparatively fast convergent characteristics.

Key Words: Adaptive Analysis, Error Estimate, Nodal Relocation Method (r-method), Size Error, Distortion Error, Finite Element Method

1. Introduction

The finite element method, being used with ease and giving comparatively correct results, has become an important tool for the analysis and design of engineering problems. It has long been realized, however, that the quality of finite element solutions greatly depends on the element discretization methods.

For this reason, many authors (Babuska et al., 1986; Lee and Bathe, 1993; Zienkiewicz and Zhu, 1987) have concentrated their efforts on the evaluation of the element discretization error. Especially, Zienkiewicz-Zhu's error estimator (Zienkiewicz and Taylor, 1989; Zienkiewicz and Zhu, 1987) for the elliptic type problems has received a lot of interest. It estimates the discretization error of finite elements through comparing the finite element stress solution with a modified continuous stress solution.

The nodal relocation method (Diaz et al., 1983; Kikuchi, 1986; Martinez and Samartin, 1991; McNeice and Marcal, 1973; Noor and Babuska, 1987; Shephard et al., 1980; Turche, 1976; Turche and McNeice, 1974) is a scheme that distributes equally the discretizing error over all elements within a given domain, by moving the nodal coordinates, thus, it is possible to generate an optimal mesh with a fixed degree-of-freedom. In the 1970s, some optimization techniques were commonly applied in the r-method in order to find an optimal mesh. At that time, it was assumed that each finite element had to share an equal amount of strain energy for linear elastic problems. In 1983, a new iterative method was suggested by R. Diaz et al. using a smoothing scheme. This method was very simple and worked reasonably well for static problems. However, this method had the disadvantage of increasing the amount of calculation due to many iteration numbers. These would be the main reason why h - and p-methods are today more popular than the r-method, although these methods rapidly increase the total degrees-of-freedom. However, if the iteration numbers can be reduced enough as

*Graduate student, Department of Mechanical Design and Production Engineering, Hanyang University

**Professor, Department of Mechanical Design and Production Engineering, Hanyang University

to apply to practical problems, the r-method would be as popular as an adaptive refinement strategy.

On the other hand, severely distorted elements are often generated in the application of the r-method based on Zienkiewicz-Zhu's error or strain energy. The construction of these distorted elements is mainly due to the changes of nodal coordinates and leads to poor approximation of the finite element solution. Therefore, it is necessary to control the element shape during the relocation of nodes.

In the finite element approximations, the size and the shape of an element are the most significant factors which affect to the solutions. Generally, the discretizing error can be defined with the size and the shape distortion error of an element. Zienkiewicz-Zhu's error estimator is also capable of evaluating the discretizing error as single stress error. However, in order to control element shape in the r-method with Zienkiewicz-Zhu's error estimator, it has to be separated into the size and the distortion errors.

This paper proposes a method which separates Zienkiewicz-Zhu's error into the size and the distortion errors for a 2D 4-node isoparametric element. A modified r-method, which can be used to find a near-optimal finite element mesh and to reduce greatly the computational time, is also presented using the error estimator.

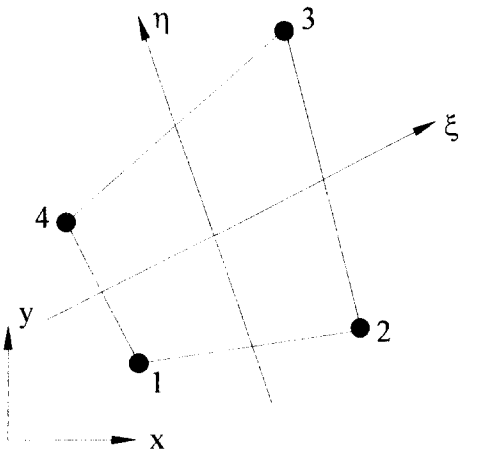

(a) Global coordinate system

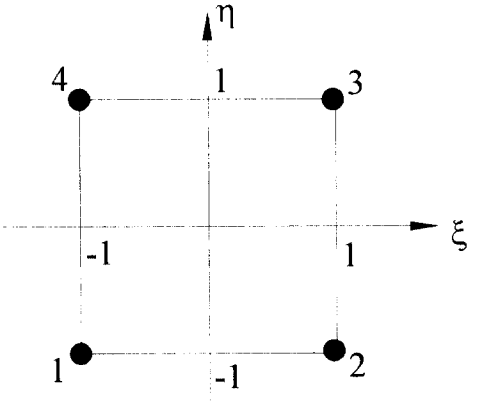

(b) Local coordinate system

Fig. 1 4-node isoparametric element and its coordinate systems

2. Definition of Discretizing Error

In order to see how to separate Zienkiewicz-Zhu's error into the size and the distortion error for the 2D 4-node isoparametric finite element, let us recall some of the essential features of the well-known isoparametric and quadrilateral elements.

2.1 Isoparametric and quadrilateral elements

2.1.1 Isoparametric element (Cook et al., 1989)

In the isoparametric element shown in Fig. 1, the shape functions can be expressed as

$$N_i^I = \frac{1}{4}(1+\xi_0)(1+\eta_0), \quad i=1, 4 \tag{1}$$

where

$$\xi_0 = \xi\xi_i \text{ and } \eta_0 = \eta\eta_i$$

and the stiffness matrix is

$$\boldsymbol{K}^I = \int_\Omega (\boldsymbol{SN}^I)^T \boldsymbol{D}\boldsymbol{S}\boldsymbol{N}^I d\Omega = \int_\Omega (\boldsymbol{B}^I)^T \boldsymbol{D}\boldsymbol{B}^I d\Omega \tag{2}$$

In the above equations, the superscript I and (ξ_i, η_i) represent the isoparametric element and the coordinates of node i in the local coordinate system, respectively; S, B and D in Eq. (2) are the partial differential operator matrix, the strain

matrix and the elastic constant matrix, respectively.

2.1.2 Quadrilateral element (Zienkiewicz and Taylor, 1989)

In the quadrilateral element shown in Fig. 2, the displacement fields can be assumed with unknown constants $a_i (i=1, 2, \cdots, 7, 8)$ as

$$u = a_1 + a_2 x + a_3 y + a_4 xy$$
$$v = a_5 + a_6 x + a_7 y + a_8 xy, \text{ or}$$
$$\boldsymbol{u} = \boldsymbol{X}\boldsymbol{a} \tag{3}$$

Substituting nodal coordinates into Eq. (3),

$$\boldsymbol{\Delta} = \boldsymbol{C}\boldsymbol{a} \tag{4}$$

we can obtain the constant vector as

$$\boldsymbol{a} = \boldsymbol{G}\boldsymbol{\Delta} \tag{5}$$

where

$$\boldsymbol{G} \equiv \boldsymbol{C}^{-1}$$

In Eqs. (4) and (5), $\boldsymbol{\Delta}$ is the nodal displacement vector, i. e., $\boldsymbol{\Delta} = [u_1\ v_1\ u_2\ v_2\ u_3\ v_3\ u_4\ v_4]^T$, and $\boldsymbol{C}$ is the constant matrix which is expressed as nodal coordinates. Simple manipulation of Eqs. (3) and (5), then, leads to the shape functions as

$$\boldsymbol{u} = \boldsymbol{X}\boldsymbol{G}\boldsymbol{\Delta} = \boldsymbol{N}^Q\boldsymbol{\Delta} \tag{6}$$

where

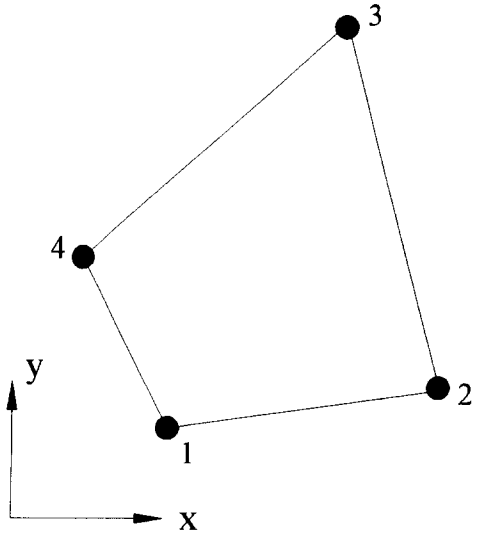

Fig. 2 4-node quadrilateral element

$$N_i^Q = G_{1i} + G_{2i}x + G_{3i}y + G_{4i}xy$$

and the stiffness matrix of a quadrilateral element can be written as

$$\boldsymbol{K}^Q = \int_\Omega (\boldsymbol{S}\boldsymbol{N}^Q)^T \boldsymbol{D}\boldsymbol{S}\boldsymbol{N}^Q d\Omega$$
$$= \int_\Omega (\boldsymbol{B}^Q)^T \boldsymbol{D}\boldsymbol{B}^Q d\Omega \tag{7}$$

In the above Eqs. (6) and (7), the superscript Q denotes the quadrilateral element and other notations are defined in Eq. (2).

2.2 Zienkiewicz-Zhu's error estimator

Zienkiewicz-Zhu's stress error can be expressed as

$$\boldsymbol{e}_\sigma = \boldsymbol{\sigma} - \hat{\boldsymbol{\sigma}} \tag{8}$$

where $\boldsymbol{\sigma}$ is the exact stress vector and $\hat{\boldsymbol{\sigma}}$ is the approximated stress vector over an element. Using this stress error, the stress error norm is computed as

$$\| \boldsymbol{e}_\sigma \|^2 = \int_\Omega (\boldsymbol{e}_\sigma)^T \boldsymbol{D}^{-1} \boldsymbol{e}_\sigma d\Omega \tag{9}$$

where Ω is the area of an element.

Zienkiewicz and Zhu approximate the exact stress vector in Eq. (8) through the nodal averaging process as follows:

$$\boldsymbol{\sigma} \cong \boldsymbol{\sigma}^* = \boldsymbol{N}\bar{\boldsymbol{\sigma}}^{av} \tag{10a}$$

$$\bar{\sigma}_i^{av} = \frac{1}{m}\sum_{e=1}^{m} (\boldsymbol{D}\boldsymbol{S}\boldsymbol{N})_i \boldsymbol{\Delta} \tag{10b}$$

where m is the number of elements surrounding node i ; $\bar{\sigma}_i^{av}$ and $\boldsymbol{\Delta}$ are the average stress vector of node i and the nodal displacement vector of element e, respectively.

2.3 Size error and distortion error of an element

In the finite element method based on the displacement, the local element displacements at any point of the 4-node isoparametric element can be assumed in the local coordinate system shown in Fig. 1 as

$$u = \gamma_1 + \gamma_2\xi + \gamma_3\eta + \gamma_4\xi\eta$$
$$v = \gamma_5 + \gamma_6\xi + \gamma_7\eta + \gamma_8\xi\eta \tag{11}$$

where γ_1-γ_8 are unknown constants. Therefore, the displacement fields of the quadrilateral element in Eq. (3) differ from those of an isopar-

ametric element depending on the shape of the element as illustrated below.

The geometric interpolations of an isoparametric element are defined by

$$x=\alpha_1+\alpha_2\xi+\alpha_3\eta+\alpha_4\xi\eta$$
$$y=\beta_1+\beta_2\xi+\beta_3\eta+\beta_4\xi\eta \tag{12}$$

where

$$\alpha_1=\frac{1}{4}(x_1+x_2+x_3+x_4)$$
$$\alpha_2=\frac{1}{4}(-x_1+x_2+x_3-x_4)$$
$$\alpha_3=\frac{1}{4}(-x_1-x_2+x_3+x_4)$$
$$\alpha_4=\frac{1}{4}(x_1-x_2+x_3-x_4)$$
$$\beta_1=\frac{1}{4}(y_1+y_2+y_3+y_4)$$
$$\beta_2=\frac{1}{4}(-y_1+y_2+y_3-y_4)$$
$$\beta_3=\frac{1}{4}(-y_1-y_2+y_3+y_4)$$
$$\beta_4=\frac{1}{4}(y_1-y_2+y_3-y_4)$$

and the physical meanings of coefficients are shown in Fig. 3.

Substituting Eq. (12) to Eq. (3), the displacement u of the quadrilateral element can be seen as :

$$\begin{aligned}u=&(a_1+a_2\alpha_1+a_3\beta_1+a_4\alpha_1\beta_1)+\{a_2\alpha_2+a_3\beta_2\\&+a_4(\alpha_1\beta_2+\alpha_2\beta_1)\}\xi+\{a_2\alpha_3+a_3\beta_3\\&+a_4(\alpha_1\beta_3+\alpha_3\beta_1)\}\eta+\{a_2\alpha_4+a_3\beta_4\\&+a_4(\alpha_1\beta_4+\alpha_2\beta_3+\alpha_3\beta_2+\alpha_4\beta_1)\}\xi\eta\\&+a_4\alpha_2\beta_2\xi^2+a_4\alpha_3\beta_3\eta^2+a_4(\alpha_2\beta_4\\&+\alpha_4\beta_2)\xi^2\eta+a_4(\alpha_3\beta_4+\alpha_4\beta_3)\xi\eta^2\\&+a_4\alpha_4\beta_4\xi^2\eta^2\end{aligned} \tag{13}$$

From Eq. (13) and Fig. 3, the coefficients α_3, α_4, β_2 and β_4 become zero in the rectangular element shown in Fig. 3(a). In this case, the transformation between the mapping coordinate system and the global coordinate system can be

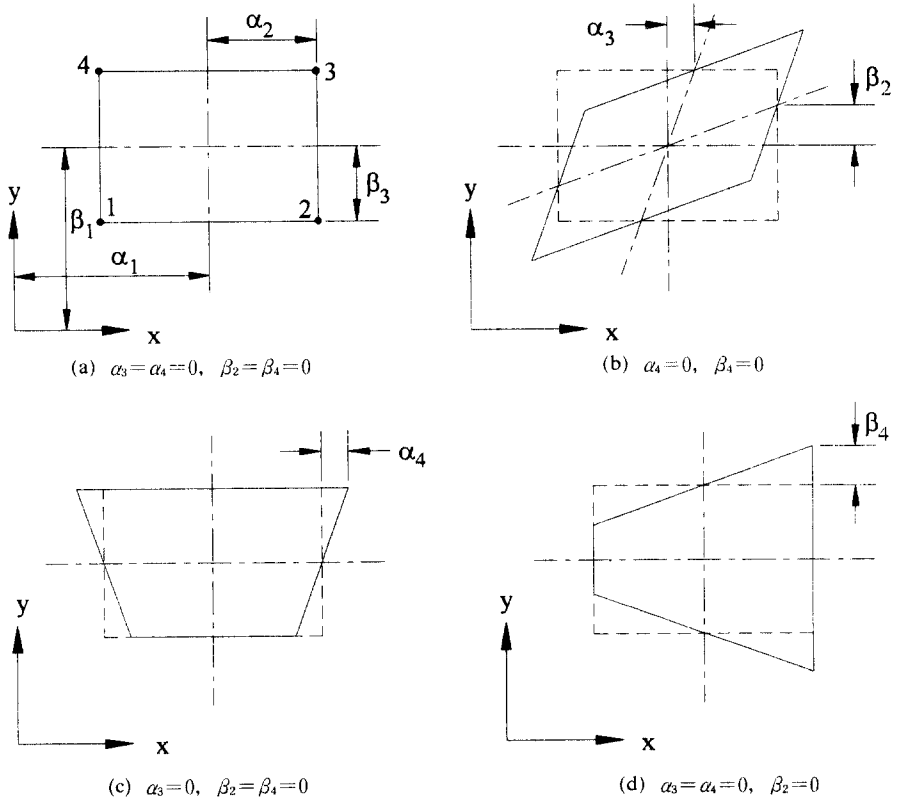

(a) $\alpha_3=\alpha_4=0$, $\beta_2=\beta_4=0$

(b) $\alpha_4=0$, $\beta_4=0$

(c) $\alpha_3=0$, $\beta_2=\beta_4=0$

(d) $\alpha_3=\alpha_4=0$, $\beta_2=0$

Fig. 3 Physical meaning of the α and β coefficients

performed exactly. However, depending on the shape (be it a parallelogram or an arbitrary shape), some of the terms ξ^2, η^2, $\xi^2\eta$, $\xi\eta^2$ and $\xi^2\eta^2$ can not be equal to zero as shown in Fig. 3(b) ~ (d). As a result, Eq. (13) differs from Eq. (11) and this causes certain error (i.e., mapping error). Therefore, we can define the discretizing error as the sum of the size and the distortion error, as given below:

The size error

$$\begin{aligned} \boldsymbol{e}_h &= \boldsymbol{\sigma}^* - \bar{\boldsymbol{\sigma}}^Q = \boldsymbol{\sigma}^* - \boldsymbol{D}\boldsymbol{B}^Q\boldsymbol{u}^Q \\ &\cong \boldsymbol{\sigma}^* - \boldsymbol{D}\boldsymbol{B}^Q\boldsymbol{u}^I \end{aligned} \tag{14}$$

and

The distortion error

$$\begin{aligned} \boldsymbol{e}_s &= \bar{\boldsymbol{\sigma}}^Q - \bar{\boldsymbol{\sigma}}^I = \boldsymbol{D}\boldsymbol{B}^Q\boldsymbol{u}^Q - \boldsymbol{D}\boldsymbol{B}^I\boldsymbol{u}^I \\ &\cong \boldsymbol{D}(\boldsymbol{B}^Q - \boldsymbol{B}^I)\boldsymbol{u}^I \end{aligned} \tag{15}$$

From Eqs. (14) and (15), the error energy norms corresponding to each error are given by

$$\| \boldsymbol{e}_h \|^2 = \int_\Omega (\boldsymbol{e}_h)^T \boldsymbol{D}^{-1} \boldsymbol{e}_h d\Omega \tag{16}$$

$$\| \boldsymbol{e}_s \|^2 = \int_\Omega (\boldsymbol{e}_s)^T \boldsymbol{D}^{-1} \boldsymbol{e}_s d\Omega \text{ and} \tag{17}$$

$$\| \boldsymbol{e}_t \| = \| \boldsymbol{e}_h \| + \| \boldsymbol{e}_s \| \tag{18}$$

where $\| \boldsymbol{e}_t \|$ represents the total error energy norm in an element due to the discretization of the domain. With these norms, it is possible to estimate the discretizing error over each element. It is noted that the size and the distortion error in Eqs. (14) and (15) are related to Zienkiewicz-Zhu's error as follows:

$$\begin{aligned} \boldsymbol{e}_\sigma &= \boldsymbol{\sigma}^* - \bar{\boldsymbol{\sigma}}^I \\ &= (\boldsymbol{\sigma}^* - \bar{\boldsymbol{\sigma}}^Q) + (\bar{\boldsymbol{\sigma}}^Q - \bar{\boldsymbol{\sigma}}^I) \\ &= \boldsymbol{e}_h + \boldsymbol{e}_s \end{aligned} \tag{19}$$

$$\begin{aligned} \| \boldsymbol{e}_\sigma \| &= \| \boldsymbol{e}_h + \boldsymbol{e}_s \| \le \| \boldsymbol{e}_h \| + \| \boldsymbol{e}_s \| \\ &= \| \boldsymbol{e}_t \| \end{aligned} \tag{20}$$

3. Node Relocation Method (r-method)

In the previous section, we discussed several error norms and derived the size and the distortion error norms. In this section, we will present how these norms can be applied to find an optimal mesh with a given initial mesh. In Sec. 3.1, we will focus on the rearrangement of nodal position in order to control element area. In Sec. 3.2, a modified r-method will be presented in order to reduce the computational time. At the end of this section, the complete modified r-method procedure will be shown.

3.1 Existing r-method

The mesh can be called optimal if all elements in the domain share an equal magnitude of error. Either Zienkiewicz-Zhu's error norm or the total error energy norm suggested in this paper may become a reasonable basis of the r-method. For the sake of convenience, we will discuss the element size redistribution strategy based on the total error energy norm.

In order to control the size of an element, we introduce the rearrangement index ξ_e of the element as

$$\xi_e = \| \boldsymbol{e}_t \|_e / \| \boldsymbol{e}_t \|_{av} \tag{21a}$$

$$\| \boldsymbol{e}_t \|_{av} = \left\{ \sum_{e=1}^{E} \| \boldsymbol{e}_t \|_e^2 \Big/ E \right\}^{\frac{1}{2}} \tag{21b}$$

where $\| \boldsymbol{e}_t \|_{av}$ and $\| \boldsymbol{e}_t \|_e$, respectively, are the average error energy norm over the domain and the total error energy norm of element e in Eq. (18); E represents the total number of elements. Therefore, the element for which ξ_e is larger than 1 should be adjusted to become smaller in size by moving its nodal coordinates, and *vice versa*. At these points, the relocation of nodes can be performed as shown in Fig. 4.

In the case of an inner node shown in Fig. 4 (a), the modification of the nodal coordinates is given by;

$$(x_i,\ y_i) = \sum_{e=1}^{m} \left\{ (\bar{x}_e,\ \bar{y}_e) \frac{\xi_e}{A_e} \right\} \Big/ \sum_{e=1}^{m} \left\{ \frac{\xi_e}{A_e} \right\} \tag{22}$$

where $\bar{x}_e$, $\bar{y}_e$ and A_e are the coordinates at the center and the area of element e respectively. Also, m represents the number of elements surrounding the node i. For the node on the boundary shown in Fig. 4(b), we introduce linear interpolation functions to be moved along the boundary as;

$$(x_i,\ y_i) = \sum_{j=1}^{2} f_j(\eta) \cdot (\bar{x}_j,\ \bar{y}_j) \tag{23a}$$

$$f_1(\eta) = \frac{1}{2}(1-\eta),\ f_2(\eta) = \frac{1}{2}(1+\eta) \tag{23b}$$

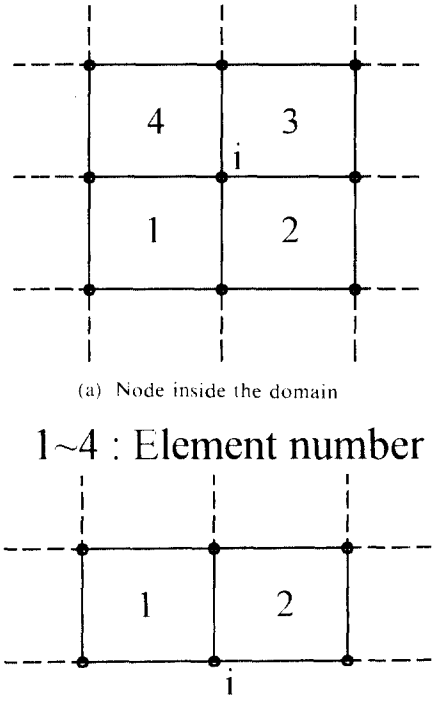

(a) Node inside the domain

(b) Node on the boundary of the domain

Fig. 4 Nodes connected with elements of the domain

$$\eta = \left(-\frac{\xi_1}{A_1} + \frac{\xi_2}{A_2}\right) \Big/ \left(\frac{\xi_1}{A_1} + \frac{\xi_2}{A_2}\right) \tag{23c}$$

where $\bar{x}_j$ and $\bar{y}_j$ are the center coordinates of an element side on the boundary of the domain.

The optimal mesh can be obtained by repeatedly applying Eqs. (22) and (23a) to each node with rearrangement indices obtained from finite element analysis, until the following convergence criteria are satisfied.

For the convergence criteria, we consider two kinds of items (i. e., the rearrangement index and displacement); convergence is indicated if

$$d_\xi^{k+1} \geq d_\xi^k \tag{24a}$$

$$u_{\max}^{k+1} \leq u_{\max}^k \tag{24b}$$

where

$$d_\xi = \left(\sum_{e=1}^{E} |1 - \xi_e|\right) \Big/ E \tag{24c}$$

In Eq. (24), the superscript k and $k+1$ are the iteration numbers; d_ξ represents the average deviation of rearrangement indices; $u_{\max}$ is the maximum nodal displacement of the domain. By the definition of d_ξ in Eq. (24c), it is said that the closer d_ξ is to the zero, the nearer a mesh is to the optimal mesh. At this point, it is possible to prevent an excessively distorted shape or large aspect ratio of an element by choosing the displacement criterion.

3.2 Modified r-method

In the r-method discussed in Sec. 3.1, an iterative scheme, which is called the 1st loop in this section, should be adopted to obtain the optimal mesh. In other words, the finite element analysis must be performed at every iteration step for the error estimation, since all elements in the domain were regenerated by modifying nodal coordinates. As a result, much of total computation time is usually consumed for the error estimate; the more total degrees-of-freedom, the more time for calculation. This may cause some difficulties when applying the r-method to practical and large problems. However, the computational time can be effectively reduced by modifying the r-method.

The basic idea is to evaluate rearrangement indices approximately without finite element computations. Then, with these approximated indices, nodal coordinates are modified by Eqs. (22) and (23). Thus, the total computation time, needed in the r-method, can be greatly reduced by repeatedly applying this process to all nodes in the domain, until certain convergence criteria are satisfied. To distinguish this iterative scheme from the 1st loop, we call this the 2nd loop in this section (See Fig. 5). We will discuss how to approximate the rearrangement index below.

Assuming that the discretizing error is proportional to the element area (Zienkiewicz and Taylor, 1989) at the k^{th} iteration in the 1st loop, the rearrangement index of the element, newly regenerated by modifying its nodal coordinates, can be approximated by

$$\xi^{j-1,k} = \frac{A^{j+1,k}}{A^{j,k}} \xi^{j,k} \tag{25}$$

where the superscript j in Eq. (25) is the number of iterations in the 2nd loop. It is noted that the rearrangement index of each element can be evaluated only with the variation of area approximately. This means that the error estimation

discussed in Sec. 2 is not necessary and, thus, the finite element analysis is not required any more for the error estimation.

Excessive applications of this process, however, may often generate severely distorted elements due to the approximation of rearrangement indices. So, we employ the following criteria based on the distortion error, given in Eq. (15), in the 2nd loop:

$$\frac{d_s^{j+1}}{d_s^j} \geq \alpha^{1/k} \text{ or } j \geq N_{\max} \tag{26}$$

where α and $N_{\max}$ are a constant and the maximum allowable number of iterations in the 2nd loop, usually $\alpha = 1.1 \sim 1.2$ and $N_{\max} = 5 \sim 7$, respectively; the superscripts k, j are the numbers of iterations in the 1st and the 2nd loops respectively; d_s is the average deviation of the distortion error, which is defined by

$$d_s = \left(\sum_{e=1}^{E} | 1 - \xi_s^e | \right) \Big/ E \tag{27}$$

where

$$\xi_s^e = \| \boldsymbol{e}_s \|_c / (\| \boldsymbol{e}_s \|_c)_{av}$$
$$\boldsymbol{e}_s \cong \boldsymbol{D}(\boldsymbol{B}^Q - \boldsymbol{B}^I)\{\boldsymbol{u}^I\}^k$$

and

$$\| \boldsymbol{e}_s \|_c^2 = \int_\Omega (\boldsymbol{e}_s)^T \boldsymbol{D}^{-1} \boldsymbol{e}_s d\Omega \quad \text{at} \quad (\xi, \eta) = (0, 0)$$

In Eq. (27), $(\| e_s \|_c)_{av}$ is the average value of $\| e_s \|_c$ for all elements in the domain; strain matrices $\boldsymbol{B}^I$ and $\boldsymbol{B}^Q$ are updated with modified nodal coordinates, but $\{\boldsymbol{u}^I\}^k$, which was obtained in the 1st loop, remains constant. It is noted that the distortion error norm $\| \boldsymbol{e}_s \|_c$ of an element is evaluated at the center point of the element in the local coordinate system. The whole procedure is shown in Fig. 5.

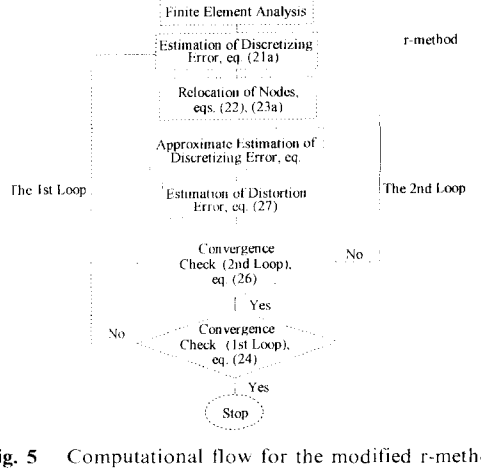

Fig. 5 Computational flow for the modified r-method

4. Numerical Examples

We now choose a series of test examples to demonstrate the effect of element shape on the discretizing error and the performance of the

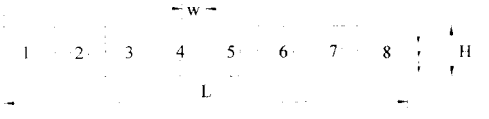

Fig. 6 Cantilever beam discretized with distorted elements (L/H = 8)

Table 1 Comparison with proposed error norms and Zienkiewicz-Zhu's error norm according to element distortion

(a) w = 0.0

	Element Number							
	1	2	3	4	5	6	7	8
S^h	1.70	1.59	1.35	1.12	0.88	0.65	0.44	0.27
S^s	0.00	0.00	0.00	0.00	0.00	0.00	0.00	0.00
S^t	1.70	1.59	1.35	1.12	0.88	0.65	0.44	0.27
S^z	1.70	1.59	1.35	1.12	0.88	0.65	0.44	0.27

(b) w = 0.2

	Element Number							
	1	2	3	4	5	6	7	8
S^h	1.07	1.04	0.86	0.71	0.55	0.40	0.26	0.16
S^s	0.59	0.63	0.53	0.43	0.34	0.24	0.14	0.04
S^t	1.65	1.67	1.39	1.14	0.89	0.65	0.41	0.20
S^z	1.69	1.67	1.34	1.10	0.87	0.64	0.43	0.27

(c) w = 0.5

	Element Number							
	1	2	3	4	5	6	7	8
S^h	1.02	0.98	0.66	0.54	0.42	0.30	0.20	0.12
S^s	1.09	0.71	0.59	0.48	0.38	0.27	0.16	0.07
S^t	2.11	1.69	1.25	1.03	0.80	0.57	0.36	0.19
S^z	2.08	2.15	1.09	0.89	0.70	0.52	0.36	0.22

modified r-method.

Figure 6 shows a cantilever beam under uniform pressure at the right end. We introduce a parameter w in order to illustrate only the effects of element shape. For each value of w, the area of an element is not changed, but only the shape of each element is changed.

The comparison of the discretizing error norms, which were separated into the size error and the distortion error in this paper, with Zienkiewicz-Zhu's error norm is given in Table 1. In Table 1, ς_h, ς_s, ς_t and ς_z are defined as

$$\varsigma_h = \| \boldsymbol{e}_h \| / \| \boldsymbol{e}_t \|_{av},\ \varsigma_s = \| \boldsymbol{e}_s \| / \| \boldsymbol{e}_t \|_{av},$$
$$\varsigma_t = \| \boldsymbol{e}_t \| / \| \boldsymbol{e}_t \|_{av} \text{ and}$$
$$\varsigma_z = \| \boldsymbol{e}_\sigma \| / \| \boldsymbol{e}_\sigma \|_{av} \tag{28}$$

where $\| \boldsymbol{e}_t \|_{av}$ and $\| \boldsymbol{e}_\sigma \|_{av}$ are average values for the total error energy norms and Zienkiewicz-Zhus error norms of all elements in the analysis domain.

In the case of rectangular elements (w=0.0) in Table 1(a), the distortion error is zero so that the

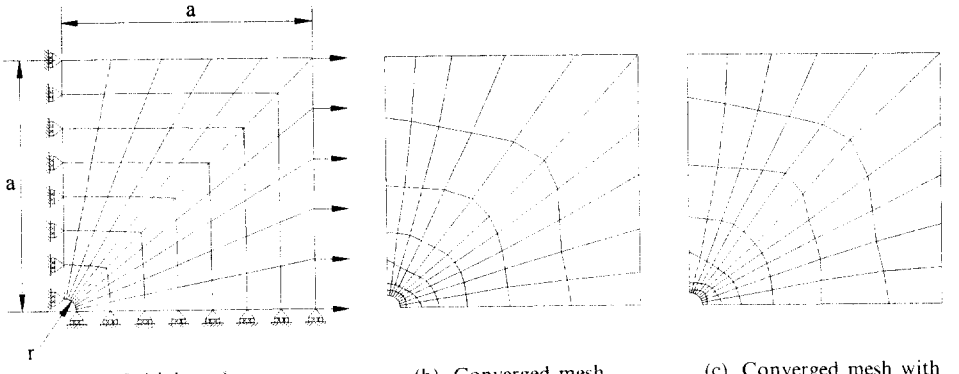

(a) Initial mesh (b) Converged mesh with r-method (c) Converged mesh with modified r-method

Fig. 7 Initial and two converged meshes for the plate with a hole (a/r=20)

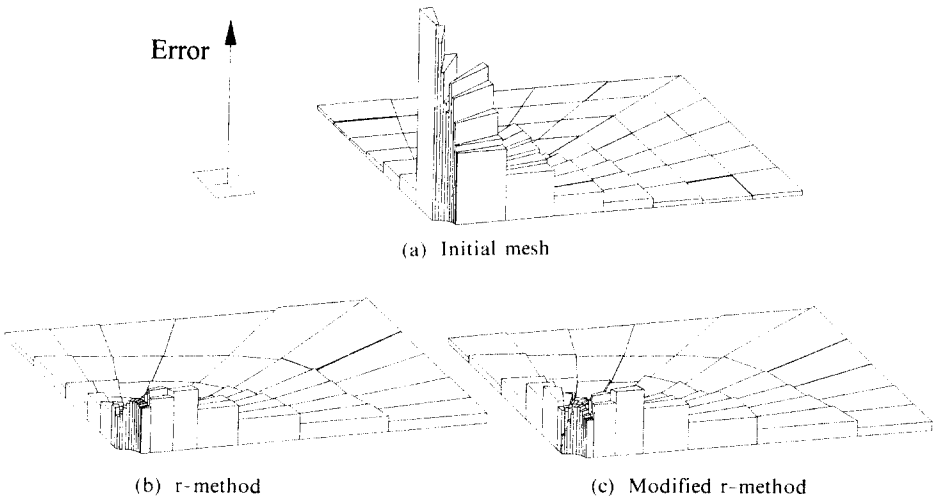

(a) Initial mesh

(b) r-method (c) Modified r-method

Fig. 8 Zienkiewicz-Zhu's error distributions of 3 kinds of meshes for the plate with a hole

Table 2 Numerical results of r- and modified r-methods for the plate with a hole

	Initial mesh	r-method	Modified r-method
Iteration Number	-	10	3
CPU Time(sec.)	-	4.72	2.03
d_s	1.19	0.52	0.59

total error energy norm and Zienkiewicz-Zhu's error norm are exactly the same. As the shape, however, of the element is distorted the distortion error increases. The total error norms which are defined by the addition of the size and the distortion error norms show similar distribution characteristics to Zienkiewicz-Zhu's error norms. Therefore, in this example, we can conclude the effects of element shape can be reasonably estimated with these distortion error norms.

In addition, it is noted that the distortion error is dependent on where the element is located in the domain. In the case of Table 1(a) or (b), all elements have a different distortion error norm, though these elements have the same distorted shapes. This is because the distortion error in this paper is based on the stress error.

The second example is the 2-D plate with a circular hole. Fig. 7 shows three kinds of meshes for this problem; Fig. 7(a) is the initial mesh and Figs. 7(b) (c), respectively, are the meshes which are obtained by the r-method and the modified r-method. These two converged meshes have similar characteristics of discretization; much larger elements are regenerated along an outer boundary, whereas smaller elements are regenerated near the hole due to stress concentration. Zienkiewicz-Zhu's error norms for each mesh are also shown in Fig. 8. In the initial mesh, the most high error norms are concentrated near the hole. However, by relocating the nodal coordinates, the distribution of these error norms is improved (i.e., initially higher error norms near the hole are rapidly reduced.). The numerical results are given

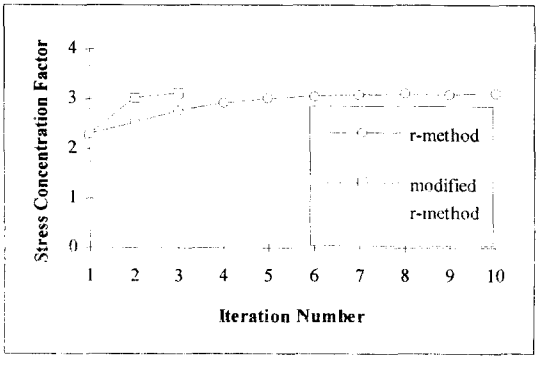

Fig. 9 Convergence of stress concentration factor for the plate with a hole

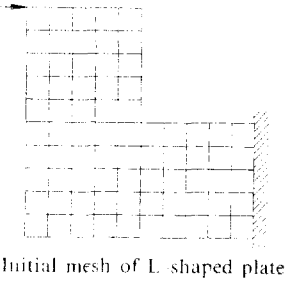

(a) Initial mesh of L shaped plate

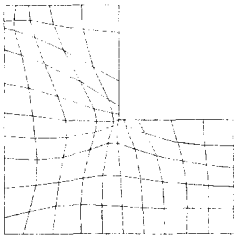

(b) Converged mesh with r-method

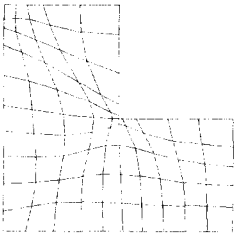

(c) Converged mesh with modified r-method

Fig. 10 Initial and two converged meshes of a L-shaped plate

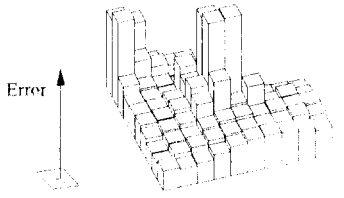

(a) Initial mesh

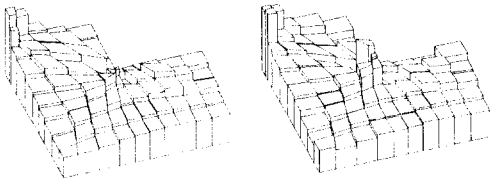

(b) r-method (c) Modified r-method

Fig. 11 Zienkiewicz-Zhu's error distributions for 3 kinds of meshes from the L-shaped plate

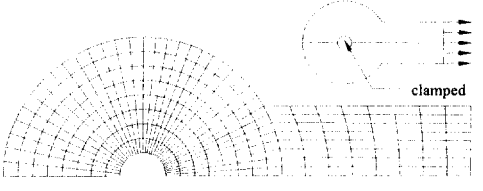

(a) Initial mesh of a lug

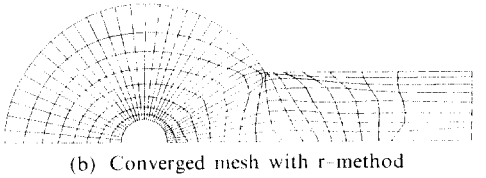

(b) Converged mesh with r-method

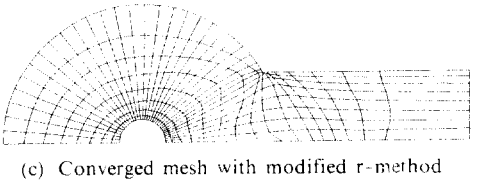

(c) Converged mesh with modified r-method

Fig. 12 Initial and two converged meshes of a lug

in Table 2 where d_s is the average deviation for the distribution of Zienkiewicz-Zhu's error norms; iteration numbers are counted in the 1st loop; CPU time based on IBM PC (Pentium -90Hz) is also given. Fig. 9 shows the stress concentration factors at the hole, and it also

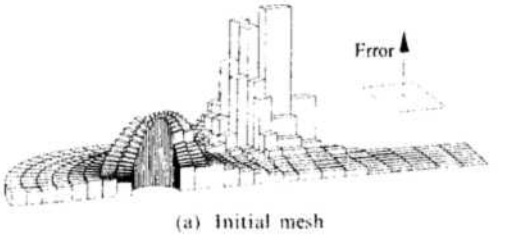

(a) Initial mesh

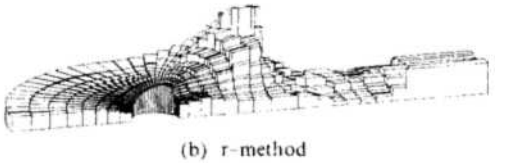

(b) r-method

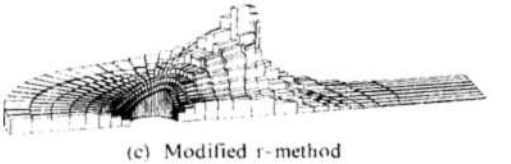

(c) Modified r-method

Fig. 13 Zienkiewicz-Zhu's error distributions for 3 kinds of meshes from the lug

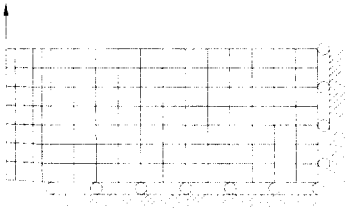

(a) Intial mesh of a cracked plate

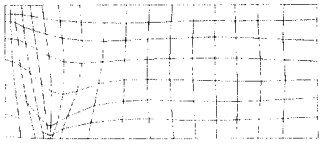

(b) Converged mesh with r-method

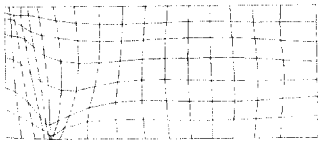

(c) Converged mesh with modified r-method

Fig. 14 Initial and two converged meshes of a cracked plate

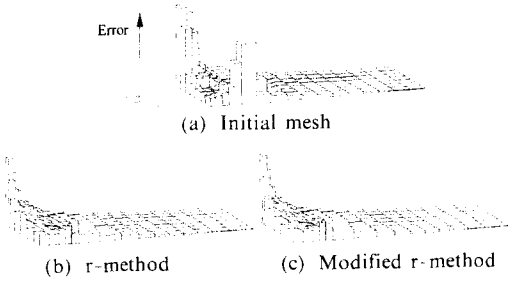

Fig. 15 Zienkiewicz-Zhu's error distributions of 3 kinds of meshes for the cracked plate

illustrates that these two r-methods can be used to improve finite element solutions. In the initial mesh, the value of the stress concentration factor at the hole is quite different with the exact value 3, but, by applying r-methods suggested in this paper, the accuracy of a solution may be greatly improved. As given in Table 2, much fewer iteration numbers and less CPU time are required in the modified r-method than in the existing r -method. Although the average deviation is slightly larger in the modified r-method than in the existing r-method, the quality of the finite element solution and the characteristics of discretization in the modified r-method are nearly the

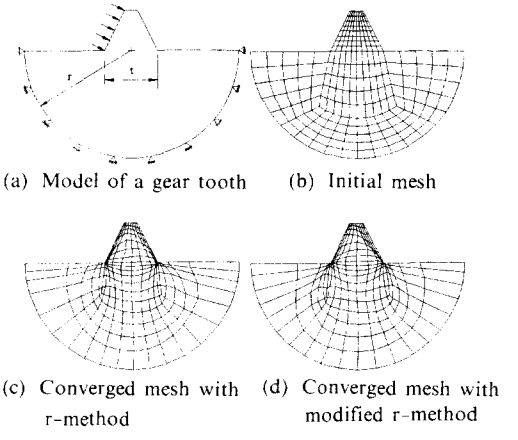

Fig. 16 Initial and two converged meshes of a gear tooth (r/t=2)

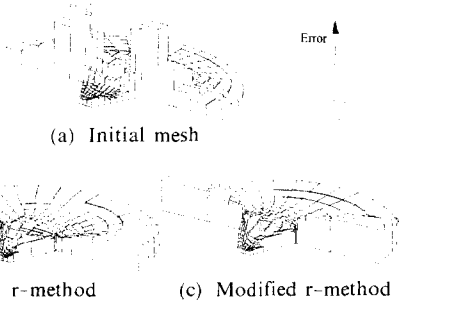

Fig. 17 Zienkiewicz-Zhu's error distributions of 3 kinds of meshes for the gear tooth

Table 3 Numerical results of r- and modified r-methods for the L-shaped plate

	Initial mesh	r-method	Modified r-method
Iteration Number	-	11	3
CPU Time(sec.)	-	5.87	2.42
d_s	0.36	0.18	0.21

Table 4 Numerical results of r- and modified r-methods for the lug

	Initial mesh	r-method	Modified r-method
Iteration Number	-	12	4
CPU Time(sec.)	-	30.70	12.85
d_s	0.65	0.42	0.48

Table 5 Numerical results of r- and modified r-methods for the cracked plate

	Initial mesh	r method	Modified r-method
Iteration Number	-	10	3
CPU Time(sec.)	-	8.62	3.84
d_s	0.87	0.80	0.82

Table 6 Numerical results of r- and modified r-methods for the gear tooth

	Initial mesh	r-method	Modified r-method
Iteration Number	-	19	5
CPU Time(sec.)	-	30.65	10.98
d_s	0.76	0.39	0.44

same as those in the existing r-method.

The results for various problems are illustrated in Figs. 10~17 and Tables 3~6. From these, we can conclude that the error norms in the initial mesh can not only be reduced more effectively, but a nearly optimum mesh can be obtained with much less computation time (about 35~45% at CPU time) by the modified r-method than by the conventional r-method.

5. Conclusions

The size and distortion error estimates, separated from Zienkiewicz-Zhu's error estimator, are presented in this paper for 2D 4-node isoparametric finite elements. These estimates can reasonably evaluate the error due to the discretization of the analysis domain, and can be easily expanded to other types of 2D finite elements, i. e., 8-node or 9-node isoparametric elements.

We can also improve the finite element solutions using the conventional r-method with this error estimator. However, there are some difficulties in the application of this r-method to practical problems because many iteration numbers are required. By modifying the r-method with the distortion error proposed in this paper, it is possible not only to reduce the number of iteration efficiently, but also to obtain the near -optimal mesh which is similar to the mesh obtained from the existing r-method.

Acknowledgment

Authors wish to acknowledge the support received from the Korean Science and Engineering Foundation through Grant No. 931-1000-037-2.

Referecnes

Babuška, I., Zienkiewicz, O. C., Gago, J. and Oliveira, E. R., 1986, *Accuracy Estimates and Adaptive Refinements in Finite Element Computations,* Wiley.

Cook, R. D., Malkus, D. S. and Plesha, M. E., 1989, *Concepts and Applications of Finite Element Analysis,* 3rd edn, Wiley.

Diaz, A. R., Kikuchi, N., Papalambros, P. and Taylor, J. E., 1983, "Design of an Optimal Grid for Finite Element Methods", *J. Struct. Mech.,* Vol. 11, No. 2, pp. 215~230.

Diaz, A. R., Kikuchi, N. and Taylor, J. E., 1983, "A method of Grid Optimization for Finite Element Methods", *Comput. Methods Appl. Meth. Eng.,* Vol. 41, pp. 29~45.

Kikuchi, N., 1986, "Adaptive Grid-Design Methods for Finite Element Analysis", *Comput. Methods Appl. Mech. Eng.,* Vol. 55, pp. 129~160.

Lee, N. S. and Bathe, K. J., 1993, "Effects on Element Distortions on the Performance of Isoparametric Elements", *Int. J. Numer. Methods Eng.,* Vol. 36, pp. 3553~3576.

Martinez, R. and Samartin, A., 1991, "Two -Dimensional Mesh Optimization in the Finite Element Method", *Comp. Struct.,* Vol. 40, No. 5, pp. 1169~1175.

McNeice, G. M. and Marcal, P. V., 1973, "Optimization of Finite Element Grids Based on Minimum Potential Energy", *J. Indust., ASME,* pp. 186~190.

Noor, A. K., Babuška, I., 1987, "Quality Assessment and Control of Finite Element Solutions", *Finite Element in Analysis and Design,* Vol. 3, pp. 1~26.

Shephard, M. S., Gallagher, R. H. and Abel, J. F., 1980, "The Synthesis of Near-Optimum Finite Element Meshes with Interactive Computer Graphics", *Int. J. Numer. Methods Eng.,* Vol. 15, pp. 1021~1039.

Turche, D. J., 1976, "On Optimum Finite Element Grid Configurations", *AIAA J.,* Vol. 14, No. 2, pp. 264~265.

Turche, D. J. and McNeice, G. M., 1974, "Guideline for Selecting Finite Element Grids Based on an Optimization Study", *Comp. Struct.,* Vol. 4, pp. 499~519.

Zienkiewicz, O. C. and Taylor, R. L., 1989, *The Finite Element Method-Basic Formulation and Linear Problems,* 4th edn, McGraw-Hill.

Zienkiewicz, O. C. and Zhu, J. Z., 1987, "A Simple Error Estimator and Adaptive Procedure for Practical Engineering Analysis", *Int. J. Numer. Methods Eng.,* Vol. 24, pp. 337~357.